

RSC Advances



This is an *Accepted Manuscript*, which has been through the Royal Society of Chemistry peer review process and has been accepted for publication.

Accepted Manuscripts are published online shortly after acceptance, before technical editing, formatting and proof reading. Using this free service, authors can make their results available to the community, in citable form, before we publish the edited article. This *Accepted Manuscript* will be replaced by the edited, formatted and paginated article as soon as this is available.

You can find more information about *Accepted Manuscripts* in the [Information for Authors](#).

Please note that technical editing may introduce minor changes to the text and/or graphics, which may alter content. The journal's standard [Terms & Conditions](#) and the [Ethical guidelines](#) still apply. In no event shall the Royal Society of Chemistry be held responsible for any errors or omissions in this *Accepted Manuscript* or any consequences arising from the use of any information it contains.

Cite this: DOI: 10.1039/c0xx00000x

www.rsc.org/xxxxxx

ARTICLE TYPE

Rhodamine-based lysosome-targeted fluorescence probes: high pH sensitivity and their imaging application in living cells†

Kang-Kang Yu,^a Kun Li,^{*a,b} Ji-Ting Hou,^a Hui-Huan Qin,^a Yong-Mei Xie,^b Chen-Hui Qian^a and Xiao-Qi Yu^{*a}

Received (in XXX, XXX) Xth XXXXXXXXXX 20XX, Accepted Xth XXXXXXXXXX 20XX

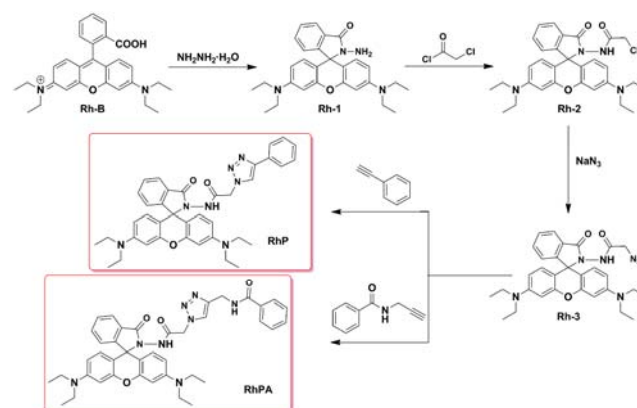
DOI: 10.1039/b000000x

Two rhodamine-based pH probes (RhP and RhPA) were synthesized *via* click reaction. The probes exhibited high pH sensitivity and selectivity with significant fluorescence intensity enhancement. Cell imaging experiments demonstrated RhPA was a good lysosomes targeting probe in living cells with low cytotoxicity and excellent photostability.

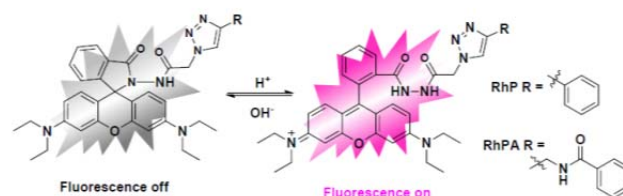
In recent years, owing to the abnormal changes of cells may cause various disease, researchers are becoming more concerned about the health state and death of living cells. As far as we know, there are plenty of ways to defined cell death, take practical microscopy approach for instance,¹ including: membrane integrity detection by DNA intercalating probes, protein expression by GFP (Green Fluorescent Protein), dielectric measurements and intracellular pH value measurements.^{2,3} Among others, intracellular pH value is widely used as an indicator for the general health of cells, and it really plays an important role in cells, such as enzyme and tissue activities, cell growth (including proliferation and apoptosis), endocytosis, multidrug resistance, calcium regulation (ion transport) and other cellular processes.⁴⁻⁹ The pH value of certain tumor tissues and organs (pH 6.0 - 6.5) possess lower compared to normal ones (pH 7.2-7.4).^{10,11} Moreover, at the cellular level, proton concentrations are not uniformly distributed: the cytoplasm is slightly alkaline (pH ~7.2), whereas the pH value of some intracellular organelles (lysosomes, endosomes and autophagosome) is in the range of 4.0 - 6.0.^{6,12-19} As the endpoint of the endocytic pathway, Lysosomes were found to be linked with the three major morphologically distinct pathways of cell death: apoptosis, type II programmed cell death and necrosis.^{20, 21} Hence, the study of sensing intracellular weakly acidic pH value, especially in lysosomes, has attracted increasing attention of researchers.

Recently, some fluorescent indicators have been developed to measure pH changes of environment or in living cells,^{5, 9} but only a few of them are suitable for pH detection in weakly acidic environments, and most of them exhibited poor membrane permeability and bad water solubility. Therefore, designing pH fluorescent probes with weakly acidic pK_a and excellent membrane permeability are still desirable. Considering that fluorescent dyes could be used for visual imaging, we intend to choose a suitable dye and prepare some lysosome-targeted pH probes. According to previous studies of other researchers, rhodamine dyes not only have excellent photostability,

photophysical properties and suitable water-solubility, but also have the potential for targeting lysosomes without introducing any other lysosome-located groups.^{15, 22-26} Since the cyclisation equilibrium in rhodamine derivatives were widely used,^{27, 28} we believe that probes based on rhodamine dyes are still of high interest, particularly for pH sensing.^{10, 29-31}



Scheme 1 Synthesis of RhP and RhPA



Scheme 2 The spirolactam ring-opening mechanism of RhP and RhPA

Herein, two rhodamine B based probes were synthesized *via* click reaction (Scheme 1). 1,2,3-triazole was introduced as an ideal bridge to improve the biocompatibility as well as water-solubility,³² moreover to avoid “alkalizing effect” we adopted benzene rather than any other aliphatic amines³³. The pH sensitive spirolactam structure of probes (RhP and RhPA) remains closed and non-fluorescent in the neutral environment; whereas weakly acidic condition leads to the ring-opening of spirolactam and the probes exhibit strong emission spectra (Scheme 2). In addition, the difference between RhP and RhPA is that RhPA comprises one more amide bond, which might serve as additional protonate groups under acid conditions. The structures of probes and intermediates were confirmed by ¹H

NMR, ^{13}C NMR and ESI-MS.

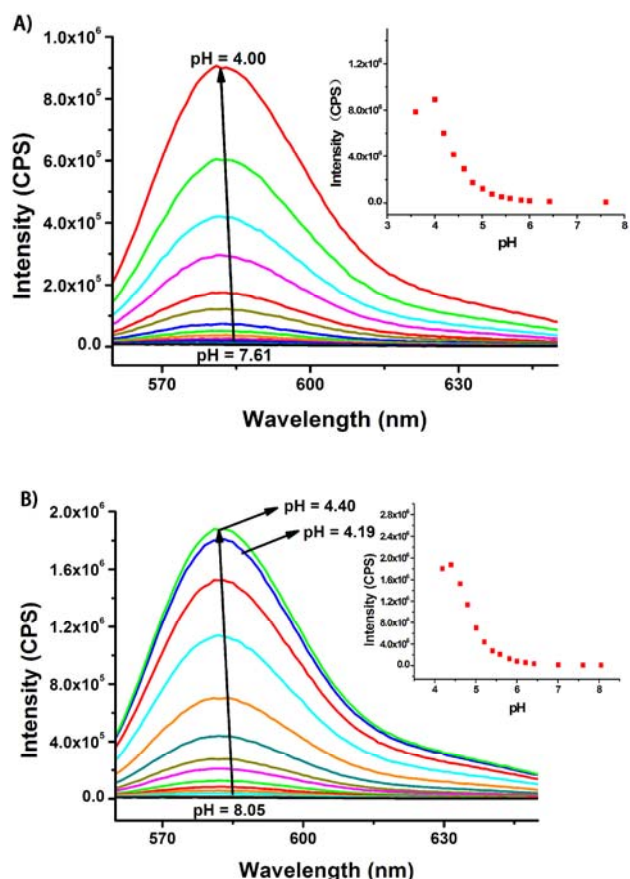


Fig. 1 A) Fluorescence spectral changes of **RhP** ($5\ \mu\text{M}$) in B-R buffer solution at different pH values ($\lambda_{\text{exc}} = 540\ \text{nm}$), and maximum emission intensity was measured at 583 nm. Inset: Plot of the emission fluorescence intensity at 583 nm. pH 3.60, 4.00, 4.19, 4.40, 4.62, 4.80, 5.01, 5.21, 5.41, 5.59, 5.82, 6.00, 6.21, 6.42, 7.01, 7.61. B) Fluorescence spectral changes of **RhPA** ($5\ \mu\text{M}$) in B-R buffer solution at different pH values ($\lambda_{\text{exc}} = 540\ \text{nm}$), and maximum emission intensity was measured at 583 nm. Inset: Plot of the emission fluorescence intensity at 583 nm. pH 3.60, 4.00, 4.19, 4.40, 4.62, 4.80, 5.01, 5.21, 5.41, 5.59, 5.82, 6.00, 6.21, 6.42, 7.01, 7.61, 8.05.

With the targeted probes in hand, we firstly investigated the fluorescent response of **RhP** and **RhPA** ($5\ \mu\text{M}$) to pH at room temperature, and Britton-Robinson buffer solution is used for turning pH values. As shown in Fig. 1, when exciting **RhP** and **RhPA** at 540 nm, non-fluorescent were found under neutral condition, while with the pH decreasing, the fluorescent intensity of the two probes increased significantly at 583 nm. **RhP** increased about 35 fold from pH 7.6 to 4.0 (Fig. 1A), and the quantum yield increased from 0.01 to 0.16; while **RhPA** increased about 75 fold from pH 8.0 to 4.4 (Fig. 1 B), and the quantum yield increased from 0.03 to 0.45. The results were definite attribute to the transformation of the ring-opened tautomer of the rhodamine fluorophore. According to the pH titration, the highly sensitive pH range of **RhP** and **RhPA** could be found to be from 4.0 to 6.0 and from 4.4 to 6.5, respectively. Moreover, the pK_{a} values of the two probes were calculated as 4.79 for **RhP** and 5.23 for **RhPA** (via the Henderson-Hasselbach-type mass action equation,³⁴ as shown in Figure S1 and Figure S2). The weak acidic pK_{a} was exactly suitable for the application

of imaging of lysosomes (intracellular acidic organelles) in living cells.

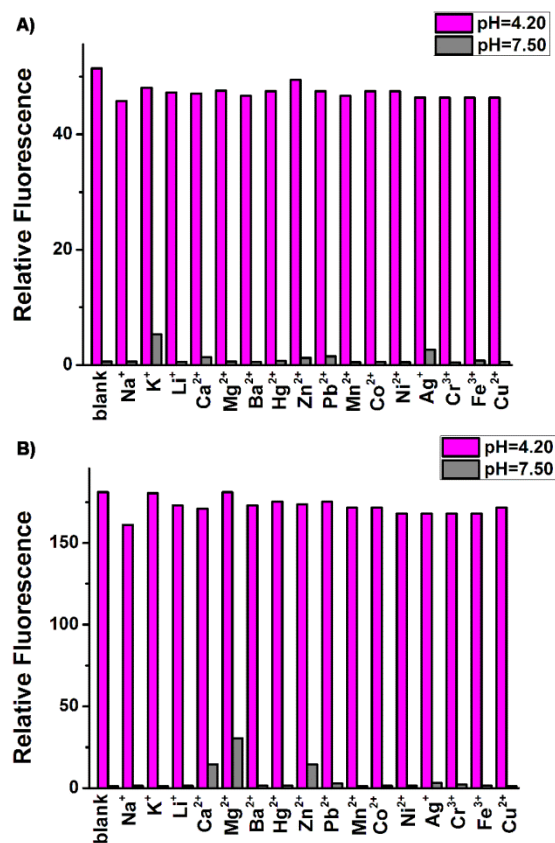


Fig. 2 A) Pink bars: Fluorescence response of **RhP** ($5\ \mu\text{M}$) at 583 nm toward other competitive ions in B-R buffer solution (pH 4.20). Grey bars: selectivity of **RhP** ($5\ \mu\text{M}$) for pH at 583 nm toward other selected interferences in B-R buffer solution (pH 7.50). B) Pink bars: Fluorescence response of **RhPA** ($5\ \mu\text{M}$) at 583 nm toward other competitive ions in B-R buffer solution (pH 4.20). Grey bars: selectivity of **RhPA** ($5\ \mu\text{M}$) for pH at 583 nm toward other selected interferences in B-R buffer solution (pH 7.50). Na^+ : 150 mM; K^+ : 75 mM; Mg^{2+} , Ca^{2+} , Zn^{2+} : 5 mM; other ions: 0.1 mM.

Subsequently, to further verify the selectivity and anti-interference of our probes, we examined the fluorescent response of **RhP** and **RhPA** for H^+ in the presence of other cations at different pH. As shown in Fig. 2, at pH = 7.50, with the addition of Na^+ (150 mM), K^+ (75 mM), Li^+ , which are plentiful in living cells; heavy and transition-metal cations such as Hg^{2+} , Pb^{2+} , Mn^{2+} , Co^{2+} , Ni^{2+} , Ag^+ , Cr^{3+} , Fe^{3+} , Cu^{2+} , no fluorescence enhancement were found for **RhP** and **RhPA**. Mg^{2+} , Ca^{2+} , Zn^{2+} (5 mM) led to feeble fluorescence enhancement of **RhPA**, however the concentration of Mg^{2+} , Ca^{2+} , Zn^{2+} *in vivo* was much lower than 5 mM, thus the effect of these ions could be neglected. Meanwhile, the influence of these metal cations was also studied at pH = 4.20, and the fluorescence intensity of **RhP** and **RhPA** in the presence of these cations were almost the same as the intensity at pH = 4.20. These results demonstrated that **RhP** and **RhPA** had high specific fluorescent response to acidic pH without any effects of the complicated intracellular condition and were suitable for imaging of living cells. Additionally, the reversibility of the sensor was also of great importance to the practical application, so we detected the reversible transformation

of our probes by pH titration. As shown in Fig. 3, an apparent decline of the fluorescence intensity of the two probes were found with the addition of OH^- (NaOH), when H^+ (HCl) was added to the solution and the pH value transferred to the original value again, the fluorescence intensity of the two probes was also recovered. This circulation could be repeated for at least ten times, and the reversible pH response would also be benefit for fluorescent intracellular pH imaging.

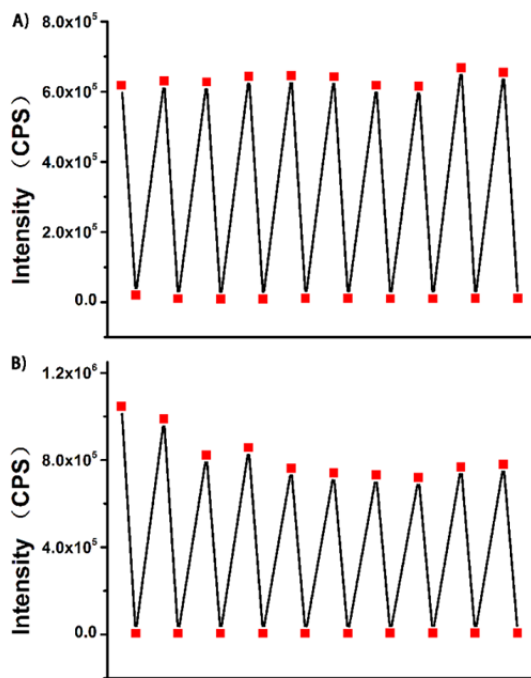


Fig. 3 A) pH reversibility research of **RhP** (5 μM) between pH ~ 4.30 and ~ 10.40 . B) pH reversibility research of **RhPA** (5 μM) between pH ~ 4.20 and ~ 10.40 .

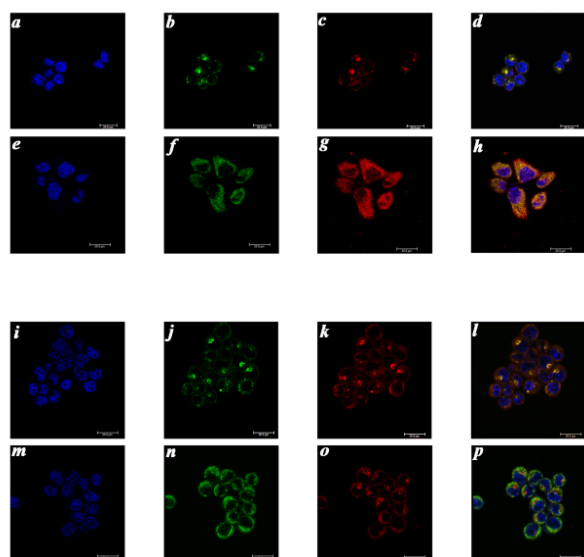


Fig. 4 Confocal microscopy images of the intracellular distribution of lysosomes (incubation 30 min). a \sim d: HeLa cells was stained with one drop NucBlue (blue channel), 1 μM LysoTracker Green (green channel) and 5 μM **RhP** (red channel). e \sim h: HeLa cells was stained with one drop NucBlue (blue channel), 1 μM MitoTracker Green (green channel) and 5 μM **RhP** (red channel). i \sim l: HeLa cells was stained with one drop NucBlue (blue channel), 1 μM LysoTracker Green (green channel) and 5

μM **RhPA** (red channel). m \sim p: HeLa cells was stained with one drop NucBlue (blue channel), 1 μM MitoTracker Green (green channel) and 5 μM **RhPA** (red channel). Blue channel: $\lambda_{\text{ex}} = 405 \text{ nm}$, $\lambda_{\text{em}} = 420 \sim 470 \text{ nm}$; green channel: $\lambda_{\text{ex}} = 488 \text{ nm}$, $\lambda_{\text{em}} = 500 \sim 540 \text{ nm}$; red channel: $\lambda_{\text{ex}} = 552 \text{ nm}$, $\lambda_{\text{em}} = 565 \sim 620 \text{ nm}$.

Finally, **RhP** and **RhPA** were applied to imaging and sensing of the pH in living cells (HeLa cells) by confocal laser scanning microscopy analysis. To determine the distribution of the probes in living cells, HeLa cells were co-stained with commercially available nucleus-specific, lysosome-specific and mitochondrion-specific staining probes, NucBlue® Live Cell Stain (one drop per milliliter), LysoTracker Green DND-26 (1 μM) and MitoTracker Green FM (1 μM). As shown in Fig. 4, the bright red emission which mainly distributed in cytoplasm indicating that **RhP** and **RhPA** could get into cells (Fig. 4 c, g, k and o). More interestingly, we noticed that the subcellular regions stained with **RhP** not only matched those stained with LysoTracker Green very well, but also matched well with MitoTracker Green staining (Fig. 4 d and h), and the subcellular regions stained with **RhPA** only matched well with LysoTracker Green staining (especially contrast l with p of Fig. 4). These preliminary results proved that **RhP** and **RhPA** had different locations in living cells.

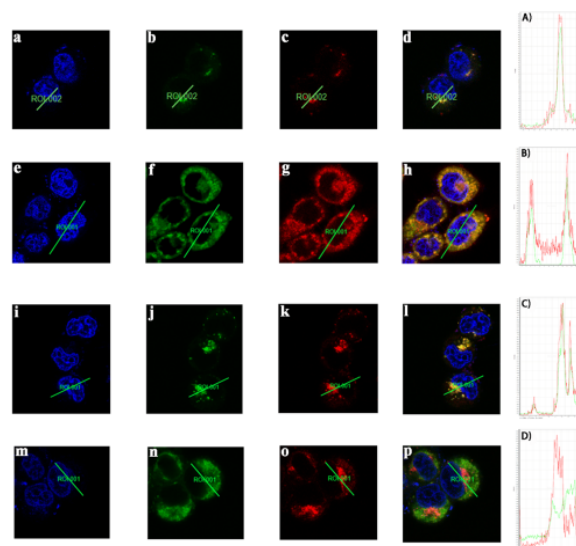


Fig. 5 a \sim d: confocal microscopy images of HeLa cells co-stained with **RhP** (5 μM), LysoTracker Green (1 μM) and NucBlue (one drop). e \sim i: confocal microscopy images of HeLa cells co-stained with **RhP** (5 μM), MitoTracker Green (1 μM) and NucBlue (one drop). i \sim l: confocal microscopy images of HeLa cells co-stained with **RhPA** (5 μM), LysoTracker Green (1 μM) and NucBlue (one drop). m \sim p: confocal microscopy images of HeLa cells co-stained with **RhPA** (5 μM), MitoTracker Green (1 μM) and NucBlue (one drop). A) \sim D): Intensity profile of regions of interest (ROI) across HeLa cells (green line – green channel, red line – red channel)

Furthermore, in order to substantiate whether only **RhPA** really could be used for lysosome (acidic compartment) specific staining, a qualitative co-localization index was measured by choosing a Region of Interest (ROI) in one cell. As Fig. 5 illustrated, the green line means the signal of LysoTracker Green and MitoTracker Green from the region we chose and the red line represents the signal of **RhP** or **RhPA** from the same region. The two coordinate graphs A) and B) of **RhP** in Fig. 5 elucidate that no matter the green line or the red line the peaks were all in the

same position, suggesting that this probe not only located in lysosomes, but also existed in mitochondria. The other two coordinate graphs C) and D) of in Fig. 5 illustrated that **RhPA** only co-stained with LysoTracker Green (the peaks of the green line and the red line were in the same position). However, although the signal from cells which co-stained with MitoTracker Green were in the same position, it is obvious that **RhPA** had strong signal intensity while MitoTracker Green exhibited weak signal intensity.

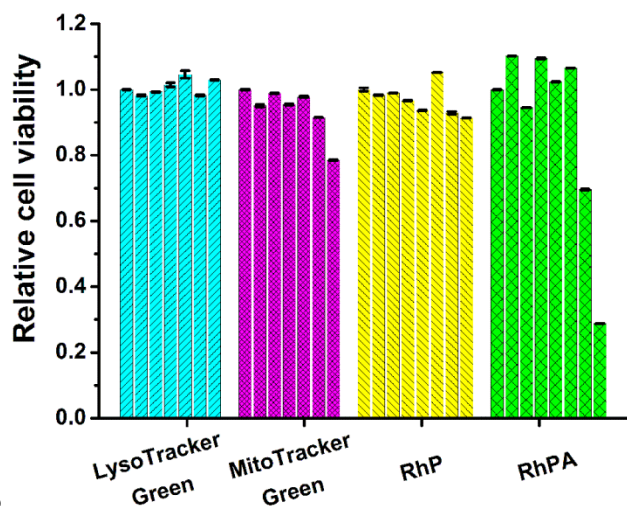


Fig. 6 Cytotoxicity of LysoTracker Green, MitoTracker Green, **RhP** and **RhPA** on HeLa cells. The concentration of LysoTracker Green and MitoTracker Green: 0 μM, 0.156 μM, 0.312 μM, 0.625 μM, 1.250 μM, 2.500 μM, 5.000 μM (from left to right). The concentration of **RhP** and **RhPA**: 0 μM, 0.625 μM, 1.250 μM, 2.500 μM, 5.000 μM, 10.000 μM, 20.000 μM, 40.000 μM (from left to right).

Besides intracellular pH imaging, the cytotoxicities of **RhP**, **RhPA** and the two commercial dyes (LysoTracker Green and MitoTracker Green) were also detected. As illustrated in Fig. 6, no obvious toxicities were found for **RhP** in cells even at the concentration of 40 μM, and no obvious toxicities were found for **RhPA** at the concentration of 10 μM. However, the two commercial dyes were more toxic. These results suggested that compared with the two commercial dyes, our probes were much less toxic, it also suggested that our probes were more beneficial for biological applications.

Conclusions

In summary, two rhodamine-based pH-sensitive probes have prepared *via* click reaction. They both have excellent selectivity and sensitivity in aqueous solution, moreover metal cations have no significant interference on pH sensing and the two probes were fully reversible mainly within the pH range from 4.2 to 10.4. **RhP** and **RhPA** exhibited low cytotoxicities and excellent photostability. The confocal co-localization imaging experiment of the two probes indicated that **RhP** and **RhPA** had good biocompatibility, and suitable for detecting the acidic region of living cells. Especially, **RhPA** could be successfully used for lysosomes targeting.

This work was financially supported by the National Program on Key Basic Research Project of China (973 Program, 2012CB720603 and 2013CB328900), the National Science

Foundation of China (Nos. 21232005, 21321061, J1310008 and J1103315), and the Specialized Research Fund for the Doctoral Program of Higher Education in China (20120181130006). We also thank the Analytical & Testing Center of Sichuan University for NMR analysis.

Notes and references

- ^aKey Laboratory of Green Chemistry and Technology, Ministry of Education, College of Chemistry, Sichuan University, Chengdu, 610064, P. R. China. Fax: (0)86-28-85415886
E-mail addresses: kli@scu.edu.cn; xqyu@scu.edu.cn
^bState Key Laboratory of Biotherapy, West China Hospital, West China Medical School, Sichuan University, Chengdu 610041, China
†Electronic Supplementary Information (ESI) available: [spectra of target probes and intermediates, detail experimental procedures]. See DOI: 10.1039/b000000x/
- C. Fink, F. Morgan and L. M. Loew, *Biophys. J.*, 1998, **75**, 1648–1658.
 - T. Aabo, J. Gluckstad, H. Siegmundfeldt and N. Arneborg, *J. R. Soc. Interface*, 2011, **8**, 1635–1643.
 - P. Patel and G. H. Markx, *Enzyme. Microb. Tech.*, 2008, **43**, 463–470.
 - Z. Diwu, C. S. Chen, C. Zhang, D. H. Klaubert and R. P. Haugland, *Chem. Biol.*, 1999, **6**, 411–418.
 - J. Han and K. Burgess, *Chem. Rev.*, 2010, **110**, 2709–2728.
 - J. R. Casey, S. Grinstein and J. Orłowski, *Nat. Rev. Mol. Cell Biol.*, 2009, **11**, 50–61.
 - M. Tantama, Y. P. Hung and G. Yellen, *J. Am. Chem. Soc.*, 2011, **133**, 10034–10037.
 - S. Chang, X. Wu, Y. Li, D. Niu, Y. Gao, Z. Ma, J. Gu, W. Zhao, W. Zhu, H. Tian and J. Shi, *Biomaterials*, 2013, **34**, 10182–10190.
 - R. Wang, C. Yu, F. Yu and L. Chen, *Trac-Trend Anal. Chem.*, 2010, **29**, 1004–1013.
 - J. Hu, X. Zhang, D. Wang, X. Hu, T. Liu, G. Zhang and S. Liu, *J. Mater. Chem.*, 2011, **21**, 19030.
 - X. Wan and S. Liu, *J. Mater. Chem.*, 2011, **21**, 10321.
 - M. I. Burguete, F. Galindo, M. A. Izquierdo, J. E. O'Connor, G. Herrera, S. V. Luis and L. Vigara, *Eur. J. Org. Chem.*, 2010, **2010**, 5967–5979.
 - Z. Li, S. Wu, J. Han and S. Han, *Analyst*, 2011, **136**, 3698.
 - H. Zhu, J. Fan, Q. Xu, H. Li, J. Wang, P. Gao and X. Peng, *Chem. Commun.*, 2012, **48**, 11766.
 - H. Lv, S. Huang, B. Zhao and J. Miao, *Anal. Chim. Acta.*, 2013, **788**, 177–182.
 - F. Miao, G. Song, Y. Sun, Y. Liu, F. Guo, W. Zhang, M. Tian and X. Yu, *Biosens. Bioelectron.*, 2013, **50**, 42–49.
 - G. Li, D. Zhu, L. Xue and H. Jiang, *Org. Lett.*, 2013, **15**, 5020–5023.
 - L. Q. Ying and B. P. Branchaud, *Bioorg. Med. Chem. Lett.*, 2011, **21**, 3546–3549.
 - P. Song, X. Chen, Y. Xiang, L. Huang, Z. Zhou, R. Wei and A. Tong, *J. Mater. Chem.*, 2011, **21**, 13470.
 - J. Stinchcombe, G. Bossi and G. M. Griffiths, *Science*, 2004, **305**.
 - B. Turk and V. Turk, *J. Biol. Chem.*, 2009, **284**, 21783–21787.
 - Z. Li, Y. Song, Y. Yang, L. Yang, X. Huang, J. Han and S. Han, *Chem. Sci.*, 2012, **3**, 2941.
 - X. Wang, R. J. Meier and O. S. Wolfbeis, *Angew. Chem. Int. Ed.*, 2013, **52**, 406–409.
 - M. H. Lee, J. H. Han, J. H. Lee, N. Park, R. Kumar, C. Kang and J. S. Kim, *Angew. Chem. Int. Ed.*, 2013, **52**, 6206–6209.

-
- 25 J. Fan, C. Lin, H. Li, P. Zhan, J. Wang, S. Cui, M. Hu, G. Cheng and X. Peng, *Dyes Pigments*, 2013, **99**, 620-626.
- 26 X. Wu, Y. Tian, M. Yu, J. Han and S. Han, *Biomaterials Science*, 2014.
- 5 27 H. N. Kim, M. H. Lee, H. J. Kim, J. S. Kim and J. Yoon, *Chem. Soc. Rev.*, 2008, **37**, 1465.
- 28 M. Beija, C. A. M. Afonso and J. M. G. Martinho, *Chem. Soc. Rev.*, 2009, **38**, 2410.
- 29 X. Wang, J. A. Stolwijk, T. Lang, M. Sperber, R. J. Meier, J. Wegener and O.S. Wolfbeis, *J. Am. Chem. Soc.*, 2012, **134**, 17011-17014.
- 10 30 H. Sun, K. Almdal and T. L. Andresen, *Chem. Commun.*, 2011, **47**, 5268.
- 31 W. Zhang, B. Tang, X. Liu, Y. Liu, K. Xu, J. Ma, L. Tong and G. Yang, *Analyst*, 2009, **134**, 367.
- 15 32 S. K. Mamidyala and M. G. Finn, *Chem. Soc. Rev.*, 2010, **39**, 1252.
- 33 H. S. Lv, J. Liu, B. X. Zhao, J. Y. Miao, *Sensor. Actust. B*, 2013, 177, 956-963.
- 34 M. Tian, X. Peng, J. Fan, J. Wang and S. Sun, *Dyes Pigments*, 2012, 20 **95**, 112-115.